JOURNAL OF MATERIALS SCIENCE 26 (1991) 6223–6230

Thermal cycling studies of a cross-plied P100 graphite fibre-reinforced 6061 aluminium composite laminate

S. MITRA, I. DUTTA, R. C. HANSEN
Materials Science Group, Department of Mechanical Engineering, Naval Postgraduate School, Monterey, CA 93943, USA

Response to thermal cycling of a 0/90 cross-plied P100 Gr-6061 aluminium composite laminate was studied between a minimum temperature (T_{min}) of 25 °C and maximum temperatures (T_{max}) of 100 and 540 °C. Strain hysteresis was observed between the heating and cooling half-cycles and was attributed to anelastic strains induced by matrix residual stresses. A residual plastic strain was also observed after the first cycle, and was seen to disappear after subsequent cycles. Alteration of the thermal residual stress state of the matrix via heat treatments was found to change significantly the magnitude of the plastic strain. These results were compared with those of studies on unidirectionally reinforced P100 Gr-6061 aluminium composites, and the differences were explained on the basis of the residual stresses resident in the matrix. Optical and electron microscopy were also utilized to observe thermal damage, which occurred predominantly along improperly bonded fibre–matrix interfaces.

1. Introduction

It is well known that large thermal residual stresses are induced in graphite–aluminium composites during cooling from the fabrication temperature due to the large difference between the longitudinal coefficients of thermal expansion (CTE) of graphite ($\sim -1 \times 10^{-6}\,°C^{-1}$) and aluminium ($\sim 22 \times 10^{-6}\,°C^{-1}$) [1–4]. These residual stresses can have a substantial effect on the thermal cycling response of the composite, resulting in strain hysteresis between the heating and cooling segments of the cycle and the generation of a residual plastic strain [5–8]. Thermal cycling of unidirectionally reinforced P100 graphite fibre-reinforced 6061 Al composites showed hysteresis and residual plastic strain, both of which were attributed to matrix yielding at the extremities of the thermal cycle [6–8]. Progressive ageing and strain hardening of the matrix were thought to be responsible for the observed disappearance of hysteresis with continued cycling [6–8]. Plastic yielding of the matrix due to applied thermal loads was also observed in other composite systems [9–11]. Dimensional changes in various as-thermally cycled composite systems have been modelled in several studies [5, 12–15]. Theoretical studies of + 26/ − 26 laminates P100 Gr–6061 Al composites, assuming only elastic unloading during the heating segment, showed no hysteresis during cycling between 24 °C (75 °F) and 121 °C (250 °F) [5], suggesting that plastic yielding is necessary for hysteresis. Additionally, visco-plastic yielding (creep) during thermal cycling has been observed in unidirectional graphite–aluminium [16] and graphite–magnesium composites [17], indicating that the strains induced during thermal cycling are heating and cooling rate dependent.

In spite of the abundance of published literature on thermal cycling of composites, no detailed explanation of the strain response based on the nature of the matrix residual stress state in various temperature regimes is available to date. In addition, none of the above studies accounts for the role of the fibre–matrix interface on the cumulative thermal damage, although interfaces are known to have a strong effect on the mechanical properties of the composite and have been observed to deteriorate with extended exposure to temperatures around 500 °C and greater [18–24]. Several investigations on the effect of thermal excursions on composite interfaces have been reported to date [25–28], although the thermal strain response of the composite was not studied in any of these works. Furthermore, most of the experimental data available in the current literature are based on unidirectionally reinforced composites, and the thermal strain response of multi-ply laminates (with different fibre orientations in contiguous plies) is not well documented.

Accordingly, the goals of this paper are three-fold: first, to study the thermal strain response of multi-ply Gr/Al composite laminates and the dependence of this behaviour on the thermal load amplitude; second, to offer an explanation of this behaviour based on the specific nature of the thermal stress state of the matrix at various stages of the thermal cycle; and finally, to investigate the role of the fibre–matrix interface on damage accumulation during thermal cycling.

0022–2461/91 $03.00 + .12

2. Experimental procedure

A 40 vol % P100 graphite fibre-reinforced 6061 Al composite laminate was used in this study. The composite lay-up consisted of seven plies in the 0/90 (cross-ply) orientation, with a total thickness of 2.2 mm. The material was manufactured using the Ti–B vapour deposit process [29, 30] in conjunction with diffusion bonding. Narrow strips (5.5 mm wide and 25.4 mm long) were cut from the as-received composite using electric discharge machining, and the edges were polished to a 1 μm finish. The thermal strain response of the composite was then measured along the long axis of the samples in an Orton™ automatic recording dilatometer. The dilatometer was calibrated between 20 and 540 °C using a 25.4 mm long sample of high purity alumina with heating and cooling rates of 0.89 and 0.31 °C min^{-1}, respectively. Subsequently, the composite samples were tested between a lower limit of 25 °C and an upper limit of either 540 or 100 °C using the same heating and cooling rates as the calibration standard. All testing was done in an argon atmosphere.

To observe the damage caused by thermal cycling, 7 mm × 7 mm billets were cut from the as-received stock and the edges were polished to a 1 μm finish. The billets were then cycled in argon atmosphere between 25 °C and either 100 or 540 °C using a pneumatically controlled apparatus attached to a tube furnace. Each cycle consisted of a 30 min heating segment, followed by a 30 min cooling segment. The dwell time at the upper and lower temperatures were 10 min each . Periodically, the cycling was interrupted and a replica of a pre-determined sample edge was obtained on cellulose acetate tape. After the replica was obtained, cycling was allowed to continue. The replicas were subsequently coated with a thin film of chromium and examined under the optical microscope. After the completion of 72 cycles, the samples were extracted from the thermal cycling apparatus and inspected under the scanning electron microscope (SEM). Two additional samples were cycled for 3 and 100 cycles, respectively, and then observed using the SEM.

To estimate the damage accumulated during thermal cycling between 25 and 100 °C, when little visual evidence of damage was observed, the stiffness-loss method was used. 25.4 mm × 5.5 mm × 2.2 mm strips were cycled in the tube furnace apparatus for various number of cycles and were tested in three-point bending using a servo-hydraulic mechanical test system (MTS) equipped with a strain-gauge extensometer. In addition to the measurement of the elastic modulus in bending, Vicker's microhardness of the matrix was also computed to determine the extent of matrix hardening due to plastic yielding or ageing during cycling.

Finally, transmission electron microscopy (TEM) was used to study the fibre–matrix interface before and after cycling in the tube furnace apparatus. 500 μm thick 3 mm diameter discs were cut from the as-received and as-cycled samples using electric discharge machining such that the graphite fibres were oriented parallel to the plane of the disc. The discs were pre-thinned to a thickness of 30 μm using a Gatan™ dimpler, followed by final thinning in a Gatan™ ion mill equipped with a liquid-nitrogen cold stage at a gun voltage of 5 kV, gun current of 1 mA and sample-to-beam inclination of 12°. The samples were then observed in a Jeol 100CX TEM equipped with a LaB_6 gun at an accelerating voltage of 120 kV. The matrix microstructures of the as-received and the as-cycled composites were also examined, and both were found to be in the overaged state.

3. Residual stress state of the matrix

The importance of matrix residual stresses in composites has led to several efforts to measure them using X-ray diffraction and other techniques. All the studies show that the matrix stresses in both longitudinal (parallel to the fibre-axis) and transverse (perpendicular to the fibre-axis) directions in unidirectional graphite–aluminium composites are tensile in nature [1–4], although the transverse stresses are somewhat smaller.

The nature of the measured stresses in unidirectional plies can be utilized to deduce the residual stress state in cross-plied composite laminates. On cooling a 0/90 cross-plied Gr/Al laminate (Fig. 1) from the fabrication temperature, the longitudinal ply develops a tensile matrix residual stress, σ_z^l. The transverse ply also develops a tensile stress σ_z^t in the z-direction, the magnitude of this stress being less than σ_z^l. The interaction between σ_z^l and σ_z^t alters the magnitudes of σ_z^l and σ_z^t somewhat. The overall matrix stress in the z-direction, however, remains tensile. The stress state in the y-direction can be deduced similarly, and it can also be shown to be tensile. For a long, narrow strip like the sample used for strain measurements in the dilatometer, the tensile stress in the z-direction (parallel to the long dimension of the sample) is the predominant component affecting the measured strain response of the composite, and will henceforth be referred to as the longitudinal stress.

4. Results and discussion

4.1. Thermal strain response

Fig. 2 shows plots of the longitudinal thermal strain response of the laminates between 25 and 540 °C for the first, second and tenth cycles. Two distinct features are immediately apparent from the figure: first, the

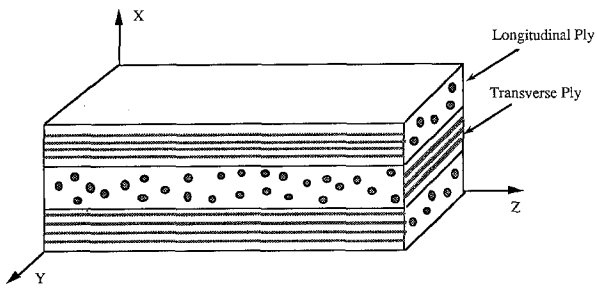

Figure 1 Schematic illustration of a continuous fibre-reinforced 0/90 cross-plied composite laminate showing the longitudinal and transverse plies and the reference coordinate system.

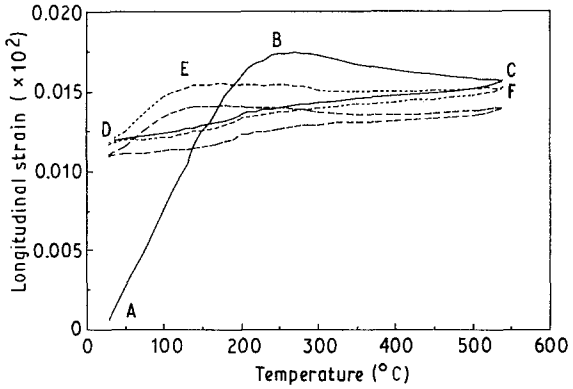

Figure 2 Thermal strain response of the as-received P100 Gr-6061 Al cross-plied composite for the (——) first, (- - -) second and (— — —) tenth cycles between 25 and 540 °C. Note the large residual plastic strain after the first cycle (A–D), and the strain hysteresis between the heating (A–B–C) and cooling (C–D) half-cycles.

existence of a distinct strain hysteresis; second, the presence of a large tensile residual plastic strain (A–D) after the first cycle. With continued cycling, the residual plastic strain is significantly reduced, although little perceptible change is observed in the strain hysteresis.

The hysteresis can be attributed to the stress state of the matrix, as outlined below. During initial heating (A–B), the longitudinal tensile stress present in the matrix aids the expansion of the composite, resulting in a CTE of about $1.1 \times 10^{-6}\,°C^{-1}$. With increasing temperature, the tensile stress is progressively relieved. After complete relief of the tensile stress, a compressive stress starts building up, resulting in a change in the sign of the composite CTE through 250 °C (B), where it is ~ 0 °C. Continued heating above 250 °C (segment B–C) induces a compressive longitudinal stress in the matrix, which opposes further expansion of the composite. This leads to the observed negative CTE in this temperature range. The build-up of the compressive stress, however, is limited by relaxation mechanisms operative at the relatively high temperature. Because the compressive stress never reaches a very large magnitude, it is quickly relieved on cooling from C (540 °C), while simultaneously assisting contraction. Eventually, a tensile stress builds up, leading to tensile yielding. Finally, a tensile residual stress is present at 25 °C (D). This tensile stress is significantly smaller than the tensile residual stress present before the first cycle because the slow heating and cooling rates result in considerable stress relaxation during the cycle. The combined effect of the tensile stresses (which aid expansion while opposing contraction) and the compressive stresses (which yield the opposite effect) prevents superposition of strains during heating and cooling, resulting in the observed strain hysteresis. The hysteresis is further enhanced by plastic deformation during the cooling half-cycle.

The residual plastic strain observed after the first cycle (Fig. 2) is indicative of overall tensile yielding of the matrix and can be explained as follows. During heating, while the longitudinal tensile stress gets progressively relieved, some tensile creep deformation can occur. Beyond 250 °C, some compressive yielding can also occur, although it is limited by the operative visco-plastic relaxation mechanisms which prevent the build-up of a large compressive stress. During cooling, the compressive stress is relieved quickly, and when the tensile stress builds up sufficiently, tensile yielding occurs. It is to be realized that because of the slow heating and cooling rates involved, matrix creep plays an important role during the entire cycle, thereby keeping the stress levels low while contributing to the observed permanent deformation. The net effect of the plastic and visco-plastic deformations is a tensile plastic strain at the end of the first cycle.

Subsequent cycling starts with a smaller tensile residual stress, leading to unloading at a lower temperature (E) than in the first cycle. Beyond E (Fig. 2), a compressive longitudinal stress attempts to build up progressively up to 540 °C (F), but is relieved by visco-plastic deformation, resulting in a net compressive plastic strain. On cooling from 540 °C, any residual compressive stress is relieved first, followed by the build-up of a tensile longitudinal stress, which can result in a small tensile plastic strain. The overall strain during the second cycle, however, is negligible, as seen in Fig. 2. With continued cycling, the tensile longitudinal residual stress resident in the matrix at the start of each cycle is lowered due to recovery mechanisms operative during the previous cycle. This results in the gradual downward shift of the strain versus temperature plot, although the magnitude of the strain hysteresis remains unaltered.

Fig. 3 plots the thermal strain response of the composite during cycling between 25 and 100 °C for the first, second and tenth cycles. Once again, a tensile residual plastic strain (A–C) is observed after the first cycle, but disappears in subsequent cycles. A prominent strain hysteresis is also observed, with the strains during cooling being larger than those during heating. Unlike the residual strain, the hysteresis is present even after ten cycles.

During the heating segment A–B, the tensile residual stress initially present in the matrix aids expansion, while being progressively relieved. Complete

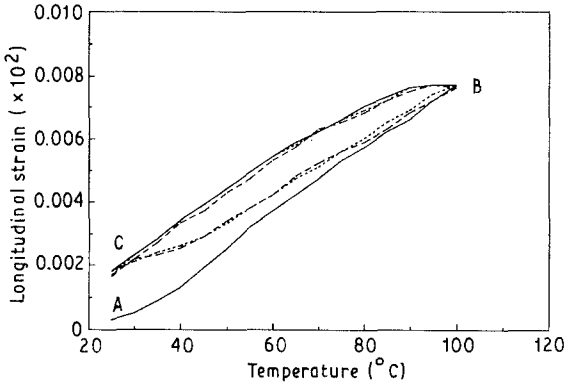

Figure 3 Thermal strain response of the as-received composite for the (——) first, (- - -) second and (— — —) tenth cycles between 25 and 100 °C. Once again, a residual plastic strain (A–C) is observed after the first cycle. Hysteresis is also seen to exist between the heating (A–B) and the cooling (B–C) half-cycles.

relief, however, occurs only around 250 °C (as discussed earlier), and even at 100 °C (point B), a net tensile longitudinal stress remains in the matrix. During cooling from B–C, the small tensile residual stress present at B starts building up again. Yielding occurs when the matrix yield strength is exceeded, resulting in a net tensile strain at the end of the first cycle. At this point (C), the residual stresses are considerably smaller than those before cycling (i.e. at A), due to partial relief via plastic and visco-plastic mechanisms. This precludes further plastic deformation during subsequent cycles, resulting in the disappearance of the residual strain. This suggests that any residual strain is primarily the result of plastic yielding of the matrix, with little contribution from visco-plastic deformation.

While the residual strain occurs due to plastic deformation of the matrix, the strain hysteresis observed is attributable primarily to anelastic strains which arise during cycling as a result of the residual stress state of the matrix. As discussed earlier, the longitudinal tensile residual stress aids expansion during heating and opposes contraction during cooling. This prevents the superposition of the strain versus temperature plots during the heating and cooling half-cycles, resulting in the observed hysteresis. Earlier studies of thermal cycling on unidirectional 41 vol % P100 Gr/6061 Al composites between 121 °C (250 °F) and − 121 °C (− 250 °F) showed strain hysteresis, which disappeared with continued cycling [6–8]. The hysteresis was attributed to matrix yielding, while its disappearance was thought to be due to matrix strengthening by age hardening and plastic yielding during cycling. In the present study, no matrix yielding occurred from the second cycle onwards (as evidenced by the absence of a residual plastic strain), although hysteresis remained. This confirms that the primary cause of the strain hysteresis between 25 and 100 °C in the present composite is not plastic deformation, but thermal stress-induced anelastic strain response during cycling.

TEM was used to observe the starting matrix microstructure of the as-received composite, and revealed a mixture of incoherent precipitate rods (15–20 nm diameter) and some platelets, clearly indicative of an overaged state. Continued cycling between 25 and 100 °C resulted in further overageing, as evinced by the decrease in matrix microhardness with cycling (Fig. 4). Two features of Fig. 4 are to be noted. First, no discernible hardening of the matrix occurred due to plastic deformation during the first cycle. Secondly, in spite of the softening of the matrix with cycling, no plastic deformation was observed in subsequent cycles. This suggests that some stress relaxation mechanism must be operative during cycling, preventing the build-up of the residual stresses beyond the matrix yield strength. The role of stress relaxation via visco-plastic recovery mechanisms during thermal exposures has been recognized by other investigators [16, 17], although it was not considered to be important in some of the earlier studies [6–8].

The other significant point to note is that residual plastic strain observed at the end of the first cycle in this study is tensile, while studies with unidirectionally reinforced composites revealed a compressive strain at the end of cycle between 25 and 121 °C [6–8]. This compressive strain was attributed to the rapid relief of the initial tensile stress by about 100 °C and the eventual generation of compressive stresses, resulting in compressive yielding at the high end of the heating half-cycle. No mention was made of the possibility of tensile strains (due to yielding or creep) between 25 and 121 °C. In this study, however, tensile strains have been conclusively shown to be present. One plausible explanation for this discrepancy is that in the present work, the longitudinal tensile residual stress in the as-received matrix was larger than that in the material used by Dries and Tompkins [6–8], preventing complete relief at 100 °C. This could be an artefact of the processing history, or because the material used in this work was cross-plied, in contradiction to the unidirectionally reinforced composite used in [6–8].

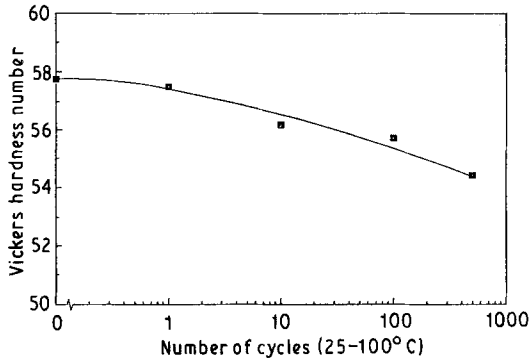

Figure 4 Plot of Vickers microhardness number (VHN) versus the number of cycles between 25 and 100 °C in argon atmosphere. The gradual decrease in microhardness is attributed to overageing of the matrix with continued cycling.

To study the effect of the matrix stress state on the strain response of the composite, thermal treatments were given to change the residual stress state prior to cycling. The samples were subjected to a stress-relief treatment at 200 °C for 4 h followed by quenching to 25 °C or − 196 °C. The heat-treatment temperature of 200 °C was chosen because most of the longitudinal tensile residual stress in the matrix is relieved at this temperature (Fig. 2). Quenching to 25 °C would then be expected to result in a relatively smaller tensile residual stress than quenching to − 196 °C.

Fig. 5 shows the thermal strain response of the sample quenched to 250 °C in the first, second and tenth cycles between 20 and 100 °C. It is observed that the average CTE for the heating segment of the first cycle ($\sim 0.9 \times 10^{-6}\,°C^{-1}$) is somewhat smaller than that for the as-received sample ($\sim 1.1 \times 10^{-6}\,°C^{-1}$), suggesting a smaller initial tensile residual stress level prior to cycling in the heat-treated sample. Only a small residual plastic strain (A–C) is noticeable. The residual strain is sharply reduced because the initial longitudinal residual stress is small enough to be substantially relieved by 100 °C, so that on cooling, the tensile stress does not build up sufficiently to cause a significant degree of plastic deformation. The hysteresis is also smaller than that in the as-received sample (Fig. 3), underlining the importance of the matrix

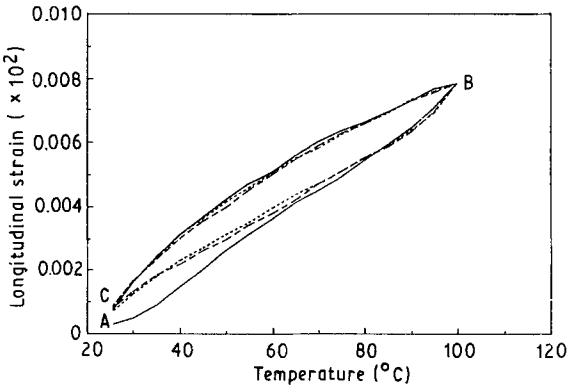

Figure 5 Thermal strain response of the composite for the (——) first, (- - -) second and (– – –) tenth cycles between 25 and 100 °C after a 4 h heat treatment at 200 °C and subsequent quenching to 25 °C. The residual strain A–C is significantly reduced, and the average CTE for the heating segment (A–B) of the first cycle is smaller than in the as-received sample (Fig. 3), indicative of smaller tensile residual stresses before cycling.

residual stress state in determining the overall strain response of the composite.

Fig. 6 shows the strain response of the sample quenched to − 196 °C. It is observed that a residual strain ($\sim 24 \times 10^{-6}$), larger than that present in the as-received sample ($\sim 17 \times 10^{-6}$; Fig. 3), is present after the first cycle. Furthermore, the average CTE for the first heating cycle is larger ($\sim 1.2 \times 10^{-6}\,°C^{-1}$) for this sample than for the sample quenched to 25 °C ($\sim 0.9 \times 10^{-6}\,°C^{-1}$) and the as-received sample ($\sim 1.1 \times 10^{-6}\,°C^{-1}$). The above observations are indicative of a larger initial tensile residual stress in this sample than in the others. Prior investigations of unidirectional 40 vol % P100 Gr/6061 Al composites have shown that the tensile residual stress induced in the matrix on quenching to − 196 °C relaxes rapidly to a small compressive value on heating the sample back to room temperature [4, 31]. The tensile strain found after the first cycle in Fig. 6, however, can only be explained if the initial residual stress was tensile. This suggests that the longitudinal tensile residual stress induced in the matrix on quenching to − 196 °C is very large in the present material, and even after relaxation on heating to 25 °C it has a large tensile value. Because the primary difference between this study and the others is that the present composite is cross-plied, it can be inferred that cross-plying retards stress relaxation during heating. The same phenomenon can be used to explain the presence of the tensile residual strain found after the first cycle between 25 and 100 °C in this study, in contradiction to the compressive strain observed by Dries and Tompkins [6–8] after cycling in the same temperature regime. In the present work, the initial tensile stress was found to be relieved around 250 °C, while in the unidirectionally reinforced composites used in [6–8] the stress was relieved around only 100 °C. This supports the hypothesis that cross-plying of composite laminates introduces additional constraints on the matrix, resulting in a higher initial longitudinal tensile stress on cooling and a slower relaxation of thermal stresses on heating.

4.2. Role of fibre–matrix interface in thermal damage

Fig. 7 shows the edge replica of a sample after three complete cycles between 25 and 540 °C in an argon atmosphere. Large cracks are evident, with the majority of cracks concentrated in regions of high fibre density. These regions of high fibre density correspond to the fibre tows which were infiltrated with liquid aluminium to form the precursor wires from which the laminate was consolidated.

In addition to the large cracks, microscopic evidence of debonding of the fibre–matrix interface was also observed. This is shown in Fig. 8, which is a scanning electron micrograph of the same sample. The fibres, which were flush with the matrix before cycling, are seen to protrude from the surface of the composite, clearly indicating interfacial separation. The majority of the observed damage occurs during the cooling half-cycle, when the graphite fibres tend to expand while the matrix tries to contract, resulting in the generation of a large interfacial shear stress. In regions where the fibre–matrix bond is not very strong, this

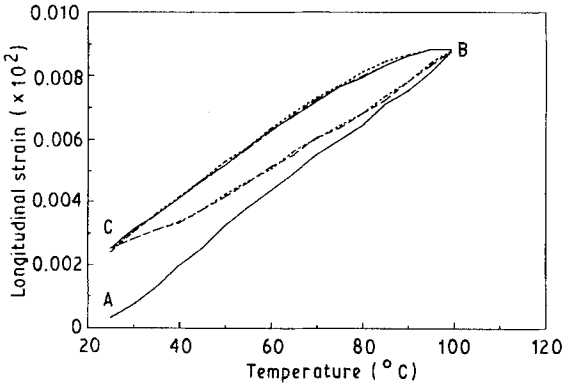

Figure 6 Thermal strain response of the composite for the (——) first, (- - -) second and (– – –) tenth cycles between 25 and 100 °C after a 4 h heat treatment at 200 °C and subsequent quenching to − 196 °C. The residual strain A–C increases to values larger than in the as-received sample (Fig. 3), while the average CTE for the heating segment of the first cycle (A–B) is also somewhat larger, suggesting large residual tensile stresses before cycling.

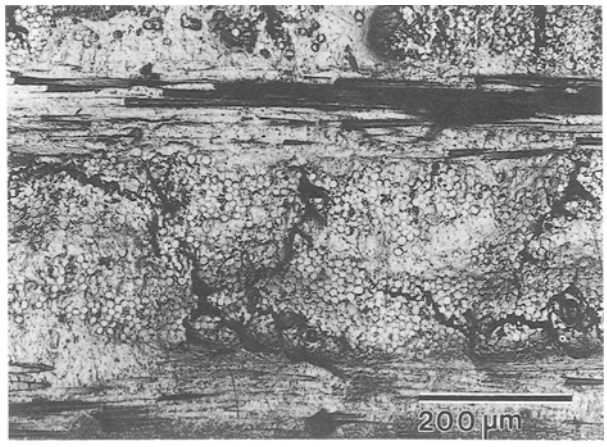

Figure 7 Photomicrograph of an edge replica of the composite after three cycles between 25 and 540 °C in argon atmosphere. Large cracks are seen in regions of high fibre density.

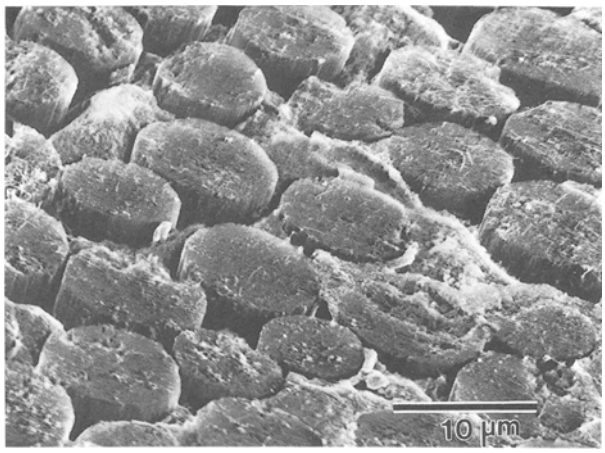

Figure 8 Scanning electron micrograph of the sample edge after three cycles between 25 and 540 °C. Fibres are observed to protrude from the matrix, indicating interfacial debonding. Debonding occurs during the cooling half-cycles when the fibres tend to expand while the matrix tends to contract.

stress can cause interfacial failure, relieving the compressive longitudinal stress in the fibre and thereby causing the fibres to protrude from the matrix. The protrusion (and hence interfacial damage) was found to become more prominent with continued cycling up to 72 cycles (Fig. 9), beyond which little additional damage was observed.

No damage was readily apparent in the sample subjected to ten cycles between 25 and 100 °C. After 100 cycles, the sample showed small interfacial cracks in regions of high fibre density, although these cracks were considerably fewer and smaller than those observed in the sample cycled between 25 and 540 °C. The gradual accumulation of damage due to cycling between 25 and 100 °C is more readily apparent from Fig. 10, which plots the bending modulus of the composite normalized by its initial value (E_b/E_b^*) with increasing number of thermal cycles. A relatively small decrease in E_b is observed initially, followed by a rapid decrease around 100 cycles and beyond. This drop in the elastic modulus is indicative of progressive damage with increasing number of cycles, and suggests that even cycling at relatively small thermal amplitudes results in interfacial damage.

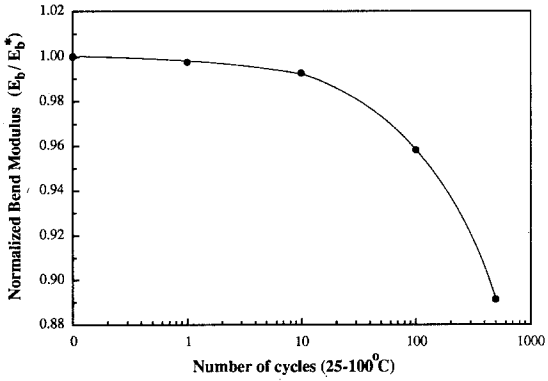

Figure 10 Plot of normalized modulus in bending (E_b/E_b^*), versus the number of cycles between 25 and 100 °C in argon. Significant loss in modulus is seen around 100 cycles and beyond, attributable to interfacial damage accumulation after extended cycling.

Selected-area diffraction patterns (SADP) taken from the fibre–matrix interface regions in the as-received composite revealed several rings corresponding to the titanium boride phase (TiB) in addition to the rings due to polycrystalline graphite. This is shown in Fig. 11, along with a centred dark-field (CDF) transmission electron micrograph of the corresponding region taken with part of the g_{401} reflection of TiB. A fine dispersion of TiB particles, 0.02–0.15 μm in size, is observed in an approximately 0.5 μm thick region adjacent to the interface. No evidence of a thin, continuous layer of TiB_2, which results from the Ti–B vapour deposit method of fabrication [29, 30], was found at the interface. The above microstructure was typical of a significant fraction of the interfacial areas studied, although several interfaces with a smooth adherent coating on the graphite fibre were also observed. Evidently, during the Ti–B vapour deposit process, where titanium and boron are co-deposited on the fibre tows to enhance wetting of graphite by

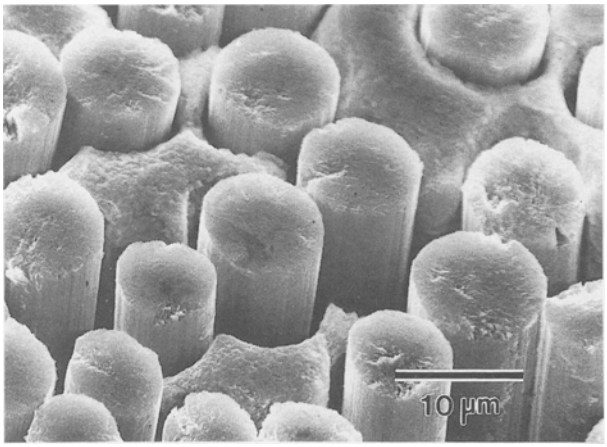

Figure 9 Scanning electron micrograph of the sample edge after 72 cycles between 25 and 540 °C in argon. A large degree of fibre protrusion is observed indicating severe interfacial damage. Beyond 72 cycles, little further increase in fibre protrusion was observed.

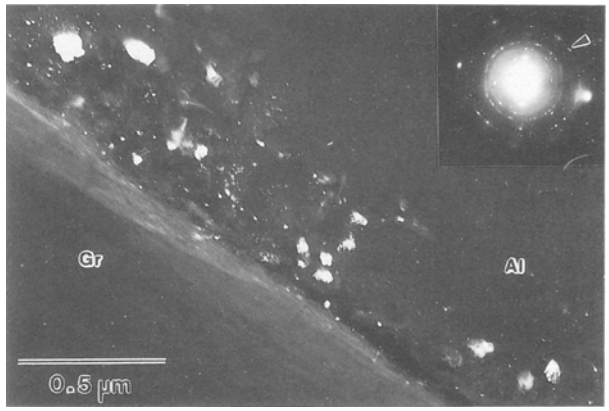

Figure 11 Selected-area diffraction pattern (SADP) and centred dark-field (CDF) transmission electron micrograph of a fibre-matrix interface in the as-received condition. The SADP shows rings due to the polycrystalline graphite fibre and the titanium boride phase (TiB). Part of the {4 0 1} ring from TiB (indicated with an arrow) was used to form the CDF image which shows numerous TiB particles (0.02–0.15 μm in size) dispersed in the matrix adjacent to the interface.

aluminium, the stoichiometry was not precisely controlled. This led to the formation of a weakly adherent layer of TiB instead of strongly adherent TiB_2. During subsequent infiltration by liquid aluminium, the TiB coating was dislodged from the fibre surface and become dispersed in the solidifying melt, thereby precluding proper wetting and good interfacial bonding. None of the interfaces examined showed any significant amount of interfacial reaction products, e.g. aluminium carbide.

The interfacial regions of the composite subjected to 72 cycles between 25 and 540 °C were also observed in the TEM. No evidence of aluminium carbide formation at the interface was discernible, strongly suggesting the absence of any chemical reaction during cycling. Although Jackson *et al.* [19] observed chemical interaction between aluminium and graphite at temperatures as low as 400 °C, it is generally recognized that extended exposure to temperatures greater than 500 °C is needed for the formation of aluminium carbide at graphite–aluminium interfaces [24]. Because the dwell time above 500 °C in each cycle during the present experiments was relatively short, extensive interfacial reaction did not occur. This indicates that any interfacial damage observed after cycling is the result of the mechanical stresses generated at the interface and not due to chemical degradation.

At this point, a mechanism can be proposed to explain the cracks observed in the as-cycled composite. During cycling, large shear stresses are generated at the interface. In regions within the fibre tows, where the interfacial coating has been disrupted during fabrication of the Al–Gr precursor wires, the bond is weak, and the shear stresses can cause local interfacial failure. The occurrence of several interfacial cracks within a small region of high fibre density allows the cracks to link up during continued cycling. This coalescence process is further aided by the microvoids which abound inside the fibre tows due to incomplete infiltration by liquid aluminium. During large amplitude cycling (25–540 °C), the majority of interfacial failure occurs within the first 70–80 cycles due to the large thermal stresses generated. Continued cycling yields little additional interfacial debonding, although damage accumulation progresses via linking-up of already existent cracks. During small amplitude cycling (25–100 °C), the stresses generated at the interface are much smaller, and interfacial debonding occurs only over a very large number of cycles. Once a statistically significant number of micro-cracks are formed at the interfaces, however, link-up occurs rapidly, leading to the rapid decline in composite stiffness observed from around 100 cycles onwards (Fig. 10).

One feature of the strain response of the composite on cycling between 25 and 540 °C was the progressive downward shift of the strain versus temperature plot with continued cycling (Fig. 2). In Section 4.1, this was attributed to the decrease in the magnitude of the tensile longitudinal stress present in the matrix before each cycle via recovery mechanisms operative during the prior cycle. Part of the stress relief, however, can also be attributed to interfacial failure during the cooling half-cycle. When some of the fibre–matrix interfaces undergo debonding, the constraint on the matrix is reduced, retarding the build-up of tensile stresses on cooling. Continued cycling causes additional debonding, resulting in the progressive depression of the strain versus temperature plot.

5. Conclusions

The thermal cycling response of a cross-plied graphite fibre-reinforced aluminium matrix composite laminate was studied in two different temperature ranges. The composite exhibited strain hysteresis during each cycle and a residual plastic strain after the first cycle in both temperature ranges. The strain hysteresis was attributed primarily to the anelastic behaviour of the matrix due to the presence of thermal residual stresses. During the first cycle, hysteresis is further enhanced by plastic deformation of the matrix. The residual plastic strain results from plastic deformation (due to both yielding and creep) and its magnitude depends on the initial matrix stress state. Altering the initial stress state of the matrix via heat treatments was found to alter the residual plastic strain appreciably. By comparing the results of the present study with earlier work [6–8], it was inferred that cross-plying has a significant effect on the initial matrix stress state and the rate of stress relaxation during heating, explaining the tensile residual strain observed after one cycle in the cross-plied composite, contrary to the compressive strain in unidirectionally reinforced materials.

Microscopic examination revealed that the principal mode of damage during thermal cycling was debonding of the fibre–matrix interface in regions of improper interfacial coating. The debonding was caused by the thermally induced interfacial shear stresses and had no contribution from chemical degradation of the interface via aluminium carbide formation. During large amplitude thermal cycling, most of the damage occurred within the first 70–80 cycles, while during small amplitude cycling, the majority of damage occurred after ~ 100 cycles. The primary effect of interfacial damage was the reduction of the thermal stresses generated during cooling due to CTE mismatch, resulting in the progressive downward shift in the strain versus temperature plot of the composite with continued cycling.

Acknowledgements

One of the authors (I.D.) gratefully acknowledges the support of this work by the Naval Weapons Support Center, Crane, IN. Additional support was provided by the NPS Research Council.

References

1. S. W. TSAI, D. MAHULIKAR, H. L. MARCUS, I. NOYAN and J. B. COHEN, *Mater. Sci. Engng* **47** (1981) 145.
2. S. D. TSAI, M. SCHMERLING and H. L. MARCUS, in "Proceedings of the 28th Sagamore Army Materials Research Conference", Bolton Landing, N.Y., July 1981, edited by E. Kula and V. Weiss (Plenum Press, 1982) p. 425.
3. H. L. MARCUS, L. RABENBERG, L. D. BROWN, G. ELKABIR and Y. M. CHEONG, in "Proceedings of the Sixth

ICCM and Second ECCM", Vol. 2, edited by F. L. Matthews, N. C. R. Buskell, J. M. Hodgkinson and J. Morton (Elsevier Applied Science, London, 1987) p. 2.459.
4. H. S. PARK, PhD Dissertation, University of Texas at Austin (1989).
5. M. H. KURAL and B. K. MIN, *J. Comp. Mater.* **18** (1984) 519.
6. G. A. DRIES and S. S. TOMPKINS, NASA TP 2402, NASA-Langley Research Center, Hampton, Virginia (1985).
7. *Idem.*, NASA TP 2612, NASA-Langley Research Center, Hampton, Virginia (1886).
8. *Idem.*, NASA TP 2701, NASA-Langley Research Center, Hampton, Virginia (1987).
9. K. G. KRIEDER and V. M. PATARINI, *Metall. Trans.* **1** (1970) 3431.
10. K. WAKASHIMA, M. OTSUKA and S. UMEKAWA, *J. Comp. Mater.* **8** (1974) 391.
11. E. G. WOLFF, in "Proceedings of the Eighth International Thermal Expansion Symposium", edited by T. A. Hahn, June 1981. (Amer. Inst. Phys., N.Y.).
12. S. NODA, N. KURIHARA, K. WAKASHIMA and S. UMEKAVA, *Metall. Trans.* **9A** (1978) 1229.
13. G. GARMONG, *ibid.* **5** (1974) 2183.
14. B. DERBY, *Scripta Metall.* **19** (1985) 703.
15. M. TAYA and T. MORI, in "Proceedings of the Sixth ICCM and Second ECCM", Vol. 2, edited by F. L. Matthews, N. C. R. Buskell, J. M. Hodgkinson and J. Morton (Elsevier Applied Science, London, 1987) p. 2.104.
16. B. K. MIN and F. W. GROSSMAN, in "Proceedings of the Eighth International Thermal Expansion Symposium", edited by T. A. Hahn, June 1981 (Amer. Inst. Phys., N.Y.) p. 175.
17. E. G. WOLFF, B. K. MIN and M. H. KURAL, *J. Mater. Sci.* **20** (1985) 1141.
18. A. A. BAKER, C. SHIPMAN and P. W. JACKSON, *Fibre Sci. Tech.* **5** (1972) 213.
19. P. W. JACKSON, D. M. BRADDICK and P. J. WALKER, *ibid.* **5** (1972) 219.
20. S. J. BAKER and W. BONFIELD, *J. Mater. Sci.* **13** (1978) 1329.
21. J. J. TRILETT, L. TERTIEN and M. BONNET-GROS, *Memb. Sci. Rev. Met.* **62** (1960) 848.
22. J. LO, D. FINELLO, M. SCHMERLING and H. L. MARCUS, in "Mechanical Behaviour of Metal Matrix Composites", edited by J. E. Hack and M. F. Amateau (TMS-AIME, Dallas, Tx. 1983) p. 77.
23. S. H. LO, S. DIONNE, G. CARPENTER and D. ZIMCIK, in "Interfaces in Metal–Ceramics Composites", edited by R. Y. Lin, R. J. Arsenault, G. P. Martins and S. G. Fishman (TMS-AMIE, Annaheim, CA. 1989) p. 165.
24. I. H. KHAN, *Metall. Trans.* **7A** (1976) 1281.
25. G. C. OLSON and S. S. TOMPKINS, in "Failure Modes in Composites-IV", edited by J. A. Cornie and F. W. Crossman (TMS-AIME, Chicago, Ill. 1979) p. 1.
26. Y. M. CHEONG and H. L. MARCUS, *Scripta Metall.* **21** (1987) 1529.
27. D. FINELLO, Y. H. PARK, M. SCHMERLING and H. L. MARCUS, in "Fractography of Ceramic and Metal Failures", edited by J. J. Mecholsky Jr and S. R. Powell Jr, ASTM STP 827 (American Society for Testing and Materials, Philadelphia, PA, 1984) p. 387.
28. Y. H. PARK and H. L. MARCUS, in "Mechanical Behaviour of Metal Matrix Composites", edited by J. E. Hack and M. F. Amateau (TMS-AIME, Dallas, Tx. 1983) p. 65.
29. W. C. HARRIGAN Jr and R. H. FLOWERS, in "Failure Modes in Composites-IV", edited by J. A. Cornie and F. W. Crossman (TMS-AIME, Chicago, Ill. 1979) p. 319.
30. M. F. AMATEAU, *J. Comp. Mater.* **10** (1976) 279.
31. M. H. RICE, A. MAEWAL and G. A. GURTMAN, "The Effects of Residual Stresses on the X-Ray Induced Response of Metal Matrix Composites", S-Cubed Corporation Technical Report SSS-FTR-89-10219, submitted to Defense Nuclear Agency (1989).

Received 23 October 1990
and accepted 25 February 1991